RSC Advances

ROYAL SOCIETY
OF CHEMISTRY

www.rsc.org/advances

1   **Molecular interaction of inorganic mercury (II) with catalase: A**

2   **spectroscopic study in combination with molecular docking**

3

4   Linfeng Chen[a], Jing Zhang[a], Yaxian Zhu[b], Yong Zhang[a,c*]

5

6   *[a] State Key Laboratory of Marine Environmental Sciences of China (Xiamen*

7   *University), College of Environment and Ecology, Xiamen University, Xiamen,*

8   *361102, China*

9   *[b] Department of Chemistry, College of Chemistry and Chemical Engineering, Xiamen*

10   *University, Xiamen, 361005, China*

11   *[c]Zhangzhou Institute of Technology, Zhangzhou, 363000, China*

12

13   *[*]Corresponding Author：*

14   Address: State Key Laboratory of Marine Environmental Science of China (Xiamen

15   University), College of Environment and Ecology, Xiamen University, 361102

16   Xiamen, Fujian Province, China.

17   Tel.: +86 592 2188685; Fax: +86 592 2888685

18   E-mail address: yzhang@xmu.edu.cn (Y. Zhang).

19
20
21
22
23
24

1 **Abstract**

2   The interaction between inorganic mercury (II) (Hg(II)) and catalase (CAT) was

3 investigated using fluorescence, UV Visible absorption (UV−Vis), circular dichroism

4 (CD) spectroscopic techniques and molecular docking methods under simulated

5 physiological conditions (in Tris-HCl buffer, pH = 7.40). The fluorescence quenching

6 analysis showed that the intrinsic fluorescence of CAT was quenched by Hg(II)

7 through a static quenching mechanism. Hg(II) can bind with CAT to form a

8 Hg(II)–CAT complex, with a binding constant of 13.24 L mol^{-1} at 295 K.

9 Thermodynamic analysis indicated that electrostatic force and van der Waals forces

10 were the dominant intermolecular forces in stabilizing the complex. The results of

11 UV−Vis absorption and CD spectral analysis indicated that the formation of the

12 Hg(II)–CAT complex induced some conformational changes in CAT, increasing and

13 decreasing its α-helical content at low and high concentrations of Hg(II), respectively.

14 The CAT activity can be inhibited by Hg(II) significantly, about a 67.2% drop with

15 the presence of 5.0×10^{-4} mol L^{-1} Hg(II), and the relative activity values of CAT

16 showed a good linear relation with its fluorescence intensity. Molecular docking was

17 employed to further investigate the interaction of CAT with different species of Hg(II)

18 (HgCl$_2$, [HgCl$_3$]$^-$ and [HgCl$_4$]$^{2-}$), to seek the optimum binding sites of Hg(II) in CAT,

19 and to obtain detailed binding information. This study contributes to the

20 understanding of the interaction mechanism between Hg(II) and CAT at the molecular

21 level *in vitro*, which is helpful for clarifying the toxicity mechanism of Hg(II) on an

22 antioxidant enzyme system *in vivo*.

1   *Keywords:* Mercury (II); Catalase; Spectroscopic methods; Molecular docking;

2   Conformational changes

3

4   **1. Introduction**

5   Catalase (CAT, EC 1.11.1.6) is one of the most important proteins of the

6   antioxidant defense system in plant and animal tissues, which can catalyze the

7   decomposition of hydrogen peroxide into molecular oxygen and water.[1, 2] Recently,

8   many studies showed that pathological states such as diabetes, aging, oxidative stress,

9   and cancer were correlated with the denaturation of CAT.[3, 4] Meanwhile, the intake of

10   contaminants is likely to influence the catalytic activity of CAT in tissues.[5] Though

11   some studies on the interactions between CAT and contaminants *in vitro* have been

12   performed,[6, 7] the toxicity mechanism of some important environmental pollutants on

13   CAT is far from being fully understood. Hence, we had paid close attention to the

14   molecular toxicity of persistent toxic substance (such as heavy metal) on CAT. To

15   understand the toxicity mechanism, we should make it clear that how the pollutant

16   bond to CAT, also the structural changes and activity inhibition of CAT induced by the

17   pollutant.

18   Mercury is one of the most toxic heavy metals presenting a serious threat with

19   respect to polluting the environment and damaging human health.[8, 9] It is known that

20   catalase in human red blood cells is responsible for the oxidation of elemental

21   mercury to divalent mercury.[10] However, inorganic mercury salts, especially mercury

1   (II) (Hg(II)) salts, are more toxic than elemental mercury due to their greater water

2   solubility.[11] Both acute and chronic exposure to Hg(II) may cause damage to organs,

3   including the lungs, kidneys, brain and liver.[12] Furthermore, mercuric chloride is the

4   most common form of Hg(II) compounds in nature.[8] Mercuric chloride intoxication

5   can cause a significant depletion of liver catalase (CAT) activity in mice.[13] Hg(II) can

6   also induce oxidative stress and make a significant contribution to the molecular

7   mechanism for liver injury.[14] Durak et al. reported that mercuric chloride can induce

8   oxidative stress in erythrocytes through the generation of free radicals and alteration

9   of the cellular antioxidant defense system.[15] However, as these reports only focused

10   on the effect of Hg(II) on CAT activity *in vivo*, little work has focused on the

11   interaction mechanisms between Hg(II) and CAT at the molecular level. Dai et al.

12   studied the interaction between mercuric chloride and bovine serum albumin by

13   spectroscopic methods at the molecular level; the binding parameters and the effect of

14   mercuric chloride on the conformation of bovine serum albumin were investigated.[9]

15   However, the mercuric chloride in Dai's experimental system actually existed as

16   different species, such as $HgCl_2$, $[HgCl_3]^-$, $[HgCl_4]^{2-}$ and so on. The assay

17   methodology within their report could not distinguish between these distinct Hg(II)

18   species. To address this underlying issue, we proposed the use of molecular docking

19   to study the binding interaction of different Hg(II) species with CAT.

20   In brief, we aimed to use spectroscopic methods combined with molecular

21   docking to study the interaction mechanism of Hg(II) with CAT *in vitro,* obtain the

4

1 binding parameters (binding constants, number of binding sites, thermodynamic

2 parameters and binding forces) of the interaction and the effect of Hg(II) on the

3 conformation of CAT, and distinguish between the interactions of CAT with different

4 species of Hg(II). By this study, we are hoping to further understand the mechanism

5 of the toxicity of Hg(II) with respect to CAT at the molecular level.

6

7 ## 2. Materials and methods

8 ### 2.1 Materials

9 Catalase (from bovine liver) was provided by Sigma Chemical Company, USA.

10 Mercuric chloride of 99.5% purity was purchased from Guizhou Tongren Chemical

11 Reagent Factory, China. H_2O_2 (30%) was purchased from Xilong Chemical Company,

12 Ltd. Tris-HCl buffer (0.05 mol L^{-1}, containing 0.10 mol L^{-1} NaCl) was used to

13 maintain the pH of the solution at 7.40. The CAT stock solution (5.0×10^{-5} mol L^{-1})

14 was prepared by dissolving CAT in Tris-HCl buffer. The mercuric chloride stock

15 solution (1.0×10^{-2} mol L^{-1}) was prepared by dissolving mercuric chloride in Tris-HCl

16 buffer. All chemicals were of analytical reagent grade, and Milli-Q water was used

17 throughout the study.

18 ### 2.2 Fluorescence spectra measurements

19 The fluorescence measurements were carried out on a Cary Eclipse fluorescence

20 spectrophotometer (Varian, USA). The excitation and emission slit widths were set to

21 5 nm and 10 nm, respectively. The excitation wavelength was set at 280 nm, and the

1   emission scans ranged from 300 to 400 nm. The excitation synchronous fluorescence

2   spectra were scanned from 260 to 310 nm ($\Delta\lambda$=15 nm) and from 250 to 310 nm ($\Delta\lambda$=

3   60 nm).

4   **2.3 UV-vis absorption measurements**

5   The UV–vis absorption spectra were measured from 200 to 500 nm at room

6   temperature (295 K) on an Agilent 8453 UV-visible spectroscopy system (Agilent

7   Technologies, USA).

8   **2.4 CD spectra measurements**

9   CD spectra were recorded from 200 to 250 nm at a scan rate of 500 nm min^{-1}

10   with a JASCO-810 spectrometer (Shimadzu, Japan). Three scans were measured and

11   averaged for each CD spectrum. All of the observed spectra were baseline corrected

12   by subtracting the spectrum of the buffer solution.

13   **2.5 CAT activity determination**

14   The activity of CAT was measured by monitoring the decrease in the absorbance

15   values at 240 nm, resulting from the consumption of H_2O_2. The relative activity of

16   CAT was calculated by the equation $\Delta A_1/\Delta A_0 \times 100\%$, where ΔA_1 and ΔA_0 are the

17   reduction of the absorption values at 240 nm in a 2-min interval after the addition of

18   CAT, with or without the presence of Hg(II), respectively.

19   **2.6 Molecular Docking Study**

20   Docking calculations were carried out with AutoDock 4.2 and the AutoDock

21   Tools (ADT) software based on the method by Xu et al.[16] The crystal structure of CAT

1 was retrieved from the Protein Data Bank (http://www.rcsb.org/pdb/home/home.do,

2 code: 1TGU). The 3D structure of ligand was generated by GaussView 5.08, and

3 optimized by DFT/B3LYP method combined with LANL2DZ basis set using

4 Gaussian 09 package. To reorganize the binding sites of the ligands in CAT, blind

5 docking was carried out by setting the grid box size to 126, 126 and 126 Å along the

6 X, Y and Z axes, with a 0.375-Å grid spacing. The Lamarckian Genetic Algorithm

7 method was applied for docking simulations. The number of Genetic Algorithm runs,

8 the population size and the maximum number of energy evaluations were set to 10,

9 150 and 250 000, respectively. For each docking case, the lowest energy docked

10 conformation was selected as the binding mode. Then, the docked conformations

11 were visualized using the PyMOL software package.[17]

12

13 **3. Results and discussion**

14 **3.1 Effect of Hg(II) on CAT fluorescence**

15 The intrinsic fluorescence of CAT arises mainly from its tryptophan (Trp),

16 tyrosine (Tyr), and phenylalanine (Phe) residues.[18] Fig. 1 shows the fluorescence

17 emission spectra of CAT with the presence of varying concentrations of Hg(II). As

18 observed from Fig. 1, pure CAT displays a strong fluorescence emission peak at 350

19 nm when excited at 280 nm, while the emission fluorescence of Hg(II) can be ignored

20 between 300 and 400 nm with identical excitation. Moreover, the fluorescence

21 intensity of CAT decreased with the addition of Hg(II), which indicated that the

1   fluorescence of CAT could be quenched by Hg(II).[19]

2   Fig. 1 should be inserted here.

3   **3.2 Fluorescence quenching mechanisms**

4   Fluorescence quenching can be caused by a dynamic or static quenching

5   process.[16, 20] To interpret the quenching mechanism of Hg(II) with CAT, the

6   fluorescence quenching spectra of CAT in the presence of various concentrations of

7   Hg(II) were measured at three temperatures (295 K, 305 K and 315 K), and the

8   fluorescence intensity data were analyzed by the modified Stern–Volmer equation

9   (S1).[19, 21]

10   Fig. 2 should be inserted here.

11   The plots of $F_0/(F_0-F)$ versus $[Q]^{-1}$ are shown in Fig. 2, and the values of K_{sv}

12   (Table 1) can be calculated from the values of the slope. The quenching rate constant

13   of the biomolecule K_q was evaluated using the equation $K_q=K_{sv}/\tau_0$. The average

14   lifetime (τ_0) of a biopolymer has been reported as 10^{-8}s.[22] It can be observed in Fig. 2

15   and Table 1 that the K_{SV} values decrease at higher temperature and that the K_q is

16   greater than 2.0×10^{10} L mol^{-1} s^{-1} (the maximum dynamic quenching constant of the

17   various quenchers).[23] These results indicated that the fluorescence quenching induced

18   by Hg(II) was initiated by the formation of the Hg(II)–CAT complex.[6, 24]

19   Table 1 should be inserted here.

20   To further clarify the fluorescence quenching mechanisms, the fluorescence

21   lifetimes of the Hg(II)–CAT system were measured, and the results are shown in Table

1   2. The data were found to fit well to the double-exponential decay model with χ^2

2   values close to 1.00. With the addition of Hg(II), the average lifetimes (τ_{AV}) of CAT

3   scarcely changed. These observations further demonstrated that the quenching of CAT

4   by Hg(II) mainly followed a static mode, which was consistent with the result from

5   the Stern–Volmer equation.[7]

6   Table 2 should be inserted here.

7   **3.3 Binding constant (K_b) and number of binding sites (n)**

8   For the static quenching interaction, the K_b and n values can be obtained from the

9   double logarithm equation (S2).[25-27] The calculated K_b and n values at different

10   temperatures are shown in Table 3. The results showed that the binding constants of

11   the Hg(II)–CAT complex were 13.24, 8.90 and 8.04 L mol^{-1} at 295 K, 305 K and 315

12   K, respectively, with the numbers of binding sites all approaching 0.5. The binding

13   constants decreased at higher temperatures, which indicated that the formation of the

14   Hg(II)–CAT complex was hindered at higher temperatures. [28]

15   Table 3 should be inserted here.

16   **3.4 Determination of the binding forces**

17   To determine the binding forces between Hg(II) and CAT, the thermodynamic

18   analyses were performed based on Ross and Subramanian's theory.[29] As the

19   temperature variation range was not too wide (from 295 K to 315 K), the interaction

20   enthalpy change(ΔH) can be regarded as a constant.[24] The thermodynamic parameters

21   (the free energy change (ΔG), ΔH and the entropy change(ΔS)) can be calculated by

1　the Van't Hoff equation and the thermodynamic equation (S3).[30, 31]

2　　　Fig. 3 should be inserted here.

3　　　The ΔH and ΔS values were calculated from the slope and intercept values of the

4　plot of ln K versus $1/T$ (Fig. 3), respectively. The thermodynamic parameters of the

5　Hg(II)–CAT system are shown in Table 4. As Table 4 indicates, the values of ΔG at

6　three temperatures were all negative, which indicated that the binding process of

7　Hg(II) with CAT was spontaneous.[1] Furthermore, because the ΔH (-19.38KJ mol^{-1})

8　and ΔS (-44.57 J mol^{-1} K^{-1}) values were all negative in the binding reaction, the

9　reaction was enthalpy driven, revealing that hydrogen bonds or van der Waals forces

10　played major roles in the formation of the Hg(II)–CAT complex.[9, 32] However, from

11　the structure of the main species of Hg(II) in our experimental system (S4), hydrogen

12　bonds cannot be formed between Hg(II) and CAT. Furthermore, as the isoelectric

13　point of CAT is 5.4,[33] it should have a negative charge in the neutral pH (7.40)

14　environment. Therefore, the electrostatic force should not be negligible between the

15　negatively charged CAT and the charged species of Hg(II). Hence, it can be concluded

16　that electrostatic force and van der Waals forces both played important roles in the

17　binding reaction.

18　　　Table 4 should be inserted here.

19　**3.5 Investigation on the conformational changes in CAT**

20　　　Though it was confirmed that the binding of Hg(II) to CAT caused the

21　fluorescence quenching of CAT, it was still unknown whether the binding may affect

1   the conformation and/or micro-environment of CAT. To further evaluate this, UV–vis

2   absorption, synchronous fluorescence, and CD spectroscopy were employed.

3   **3.5.1 UV–vis absorption spectroscopy**

4   As a simple but effective method, UV-vis absorption spectroscopy can be used to

5   explore the structural changes in CAT.[5, 34] Fig. 4 shows the UV-vis absorption spectra

6   of the Hg(II) and CAT mixtures (curves c and d), CAT (curve e), and different

7   concentrations of Hg(II) (curves a and b). Fig. 4 (A) illustrates that the absorption

8   bands of Hg(II) and CAT overlap strongly at approximately 213 nm, which reflects

9   the framework conformation of CAT.[35, 36] So, the subtraction spectra (curves f and g)

10   in Fig. 4 (B) were obtained by deducting the spectra of Hg(II) from the spectra of the

11   mixed Hg(II) and CAT. It can be observed from Fig. 4 (B) that the absorption peak at

12   213 nm decreases with the addition of Hg(II), indicating that the interaction between

13   Hg(II) and CAT leads to the loosening and unfolding of the CAT skeleton.[37, 38]

14   Furthermore, the weak absorption bands around 280 nm and 405 nm were nearly

15   unchanged, which demonstrated that the binding of Hg(II) to CAT did not drastically

16   change the microenvironment around the tryptophan residues and the porphyrin ring

17   of the heme.[16, 39]

18   Fig. 4 should be inserted here.

19   **3.5.2 Synchronous fluorescence spectroscopy**

20   Synchronous fluorescence spectroscopy was further utilized to study the

21   microenvironment changes in CAT induced by Hg(II) based on the possible shift in

1   the maximum excitation wavelength.[40] When the wavelength intervals (Δλ) were set

2   as 15 nm or 60 nm, the synchronous fluorescence spectra of CAT characterized the

3   polarity changes of the tyrosine (Tyr) or tryptophan (Trp) residues of CAT,

4   respectively.[41] Fig. 5 shows the synchronous fluorescence spectra of CAT in the

5   presence of various amounts of Hg(II). As illustrated by Fig. 5, the synchronous

6   fluorescence intensity of Tyr and Trp both decreased with the addition of Hg(II), and

7   the emission peaks showed no shift over the investigated concentration range. This

8   finding indicated that Hg(II) had no obvious effect on the microenvironment of the

9   Tyr and Trp residues in CAT,[42] which was in good agreement with the conclusions

10   drawn from the UV–vis absorption spectral analysis.

11   Fig. 5 should be inserted here.

12   **3.5.3 CD spectroscopy**

13   To further understand the influence of Hg(II) on the secondary structure of CAT,

14   CD spectroscopy was used. The CD spectra of CAT in the absence and presence of

15   Hg(II) are shown in Fig. 6. As Fig. 6 indicates, the CD spectrum of pure CAT contains

16   two main negative bands at approximately 211.0 and 219.0 nm, which are

17   characteristic of the α-helical structure of the protein.[43] It was also found that with the

18   addition of Hg(II), the ellipticity of CAT changed significantly. Furthermore, the

19   CDPro software package was employed to analyze the CD spectra, and the

20   proportions of four secondary structures of CAT were obtained (Table 5). Table 5

21   shows that the secondary structures of pure CAT consist of 17.6% α-helix, 28.9%

1   β-sheet, 24.1% β-turn and 24.4% random coil. After the addition of small amounts of

2   Hg(II) to CAT (10:1,100:1), the α-helix content of CAT increased to 23.6% and 24.7%,

3   and the β-sheet content decreased to 27.4% and 23.6%. It was possible that the

4   charged Hg(II) bonded with the surface charges of the CAT, which enhanced the

5   helical structure by the dipole–dipole interaction between or within the CAT.[44]

6   However, when the molar ratio of Hg(II) to CAT increased to 1000, the α-helix

7   content decreased to 4.9% and the β-sheet content increased to 38.7% rapidly, which

8   may be because Hg(II) conjugated with certain amino acid residues within the CAT

9   and therefore destroyed its hydrogen bonding networks.[9] Meanwhile, the decrease in

10   α-helix content indicated that a high concentration of Hg(II) can cause unfolding of

11   the CAT skeleton,[45] which was in good agreement with the results of the absorption

12   study.

13   Fig. 6 should be inserted here.

14   Table 5 should be inserted here.

15   **3.6 Effects of Hg(II) on CAT activity**

16   It is well known that the structural change of a protein is closely related to its

17   biological function.[46, 47]According to the above results, the addition of Hg(II) changed

18   the conformation of CAT remarkably, but the relevant activity changes were still

19   unknown. Hence, the effects of different concentrations of Hg(II) on the activity of

20   CAT were investigated. As shown in Fig. 7, the CAT activity decreased rapidly with

21   Hg(II) concentration increasing from 0 to 5.0×10^{-4} mol L^{-1}. As the Hg(II)

1 concentration increased to 5.0×10^{-4} mol L^{-1}, the CAT activity decreased to a minimum

2 of approximately 32.8% of the initial level. This result suggested that the activity of

3 CAT decreased in the presence of Hg(II), which may be caused by the conformational

4 changes, as reported previously for a graphene oxide and CAT system.[16] Meanwhile,

5 it was likely that Hg(II) would have an acute toxic effect on an antioxidant enzyme

6 system in organisms.

7   Fig. 7 should be inserted here.

8 **3.7 Correlativity of CAT activity and CAT fluorescence intensity**

9   Both the CAT activity and the CAT fluorescence intensity decreased significantly

10 with the addition of Hg(II), and it was interesting to determine their inter-dependent

11 relation within this study. Fig. 8 demonstrates a clear linear relation between the CAT

12 activity and the CAT fluorescence intensity. The linear regression equation was

13 determined to be Y=1.36X-248.09, and the correlation coefficient (*r*) was 0.9453.

14 This phenomenon may be ascribed to the fact that both the CAT activity and CAT

15 fluorescence intensity changed mainly as a result of the conformational changes of

16 CAT.

17   Fig. 8 should be inserted here.

18 **3.8 The species of Hg(II) in the experimental system**

19   It is well known that Hg^{2+} shows a strong trend to form coordination complexes

20 with chloride ion (such as [HgCl]$^{+}$, HgCl$_2$, [HgCl$_3$]$^{-}$, and [HgCl$_4$]$^{2-}$) and hydroxides

21 (such as [HgOH]$^{+}$, Hg(OH)$_2$, and [Hg(OH)$_3$]$^{-}$).[48] The buffer solution used in our

1   experimental system contained 0.1 mol L^{-1} chloride ion, and the pH value was 7.40.

2   So, coordination equilibrium was used to calculate the contents of different Hg(II)

3   species (S4). The results suggest that the main species of Hg(II) in our experimental

4   system were HgCl$_2$, [HgCl$_3$]$^-$, and [HgCl$_4$]$^{2-}$, at 41.35%, 29.27%, and 29.27%,

5   respectively.

6   **3.9 Molecular docking**

7   It is apparent that different species of Hg(II) may have different effects on CAT.

8   However, it is difficult to determine the difference through the experimental method.

9   Hence, computational chemistry could be employed to resolve this question.[49, 50]

10   Molecular docking was used to understand the interaction of CAT with different

11   species of Hg(II) (HgCl$_2$, [HgCl$_3$]$^-$ and [HgCl$_4$]$^{2-}$).[51] For each species of Hg(II), the

12   lowest binding energy conformer was determined from 10 different conformers for

13   further investigation.[52] Fig. 9 shows the most possible interaction modes between

14   CAT and different species of Hg(II), and the related data are shown in Table 6 and

15   Table 7. Fig. 9 (A) shows that the binding sites of HgCl$_2$, [HgCl$_3$]$^-$ and [HgCl$_4$]$^{2-}$ with

16   CAT are significantly different. For HgCl$_2$, the probe molecule is surrounded by

17   amino acid residues Val 322, Glu 327, Pro 373, Val 374, Met 394, and Asp 395. The

18   probe molecule of [HgCl$_3$]$^-$ is located adjacent to amino acid residues Trp 14, Arg 18,

19   Gln 21, Asp 24, and Arg 381. In the case of [HgCl$_4$]$^{2-}$, the amino acid residues consist

20   of Pro 107, Arg 319, and Tyr 378. As shown in Table 6, electrostatic forces play a

21   more important role in the binding interactions of CAT with HgCl$_2$ and [HgCl$_3$]$^-$. In

1   contrast, the dominant binding forces for $[HgCl_4]^{2-}$ are van der Waals forces. In

2   addition, no hydrogen bonds are observed between CAT and different species of

3   Hg(II). Overall, electrostatic and van der Waals forces are the dominant

4   intermolecular forces in the binding interactions of CAT with Hg(II). The binding

5   energy values calculated from the docking studies for $HgCl_2$–CAT, $[HgCl_3]^-$–CAT and

6    $[HgCl_4]^{2-}$–CAT systems were -6.15, -3.06 and -1.92 kJ mol^{-1}, with binding constants

7   of 11.97, 3.42 and 2.17 L mol^{-1}, respectively. Meanwhile, the experimentally

8   calculated binding energy and binding constant were -6.23 kJ mol^{-1} and 13.24 L mol^{-1}

9   for the Hg(II)–CAT system. The experimental values were close to the docking values

10   of the $HgCl_2$–CAT system, which may be because the content of $HgCl_2$ was the

11   highest in the experimental system.

12   Fig. 9 should be inserted here.

13   Table 6 should be inserted here.

14   Table 7 should be inserted here.

15   In this study, firstly, fluorescence, UV–vis and CD spectra were used to obtain

16   the binding parameters of the interaction of Hg(II) with CAT and to confirm the

17   significant structural changes and activity inhibition of CAT induced by Hg(II).

18   Secondly, we focused on the fact which was too easy to be ignored that the metal ions

19   may interact with other ions or molecules and then exist as different species. In order

20   to distinguish between the interactions of CAT with different species of Hg(II),

21   molecular docking was further employed. So, this work has significant implications

1   for the research about the interactions of proteins with metal ions.

2   **4. Conclusions**

3   The above results showed that by combining multiple spectroscopic techniques

4   and molecular docking simulation methods, the interaction mechanism of Hg(II) with

5   CAT can be revealed in depth. The results indicated that Hg(II) can interact with CAT

6   to form a complex through electrostatic and van der Waals forces. Low and high

7   concentrations of Hg(II) can induce different conformational changes in CAT. The

8   CAT activity was inhibited after binding with Hg(II), and the relative activity values

9   were linearly associated with the CAT fluorescence intensity. Molecular docking

10   results revealed that different species of Hg(II) were located at different sites on CAT,

11   and detailed binding information was also explored. In conclusion, this study

12   successfully furthered the understanding of the toxicity mechanism of Hg(II) on CAT

13   at the molecular level.

14   It is well known that organic mercury is more toxic and bioavailable than

15   inorganic mercury and can be biomagnified through trophic transfer. Hence, to fully

16   understand the toxicity mechanism of mercury on an antioxidant enzyme system,

17   further research should be performed to investigate the interaction mechanism of

18   organic mercury with CAT *in vitro*.

19

20   **Acknowledgements**

RSC Advances Accepted Manuscript

3

4 References

5 1. Y. Teng, L. Y. Zou, M. Huang and W. S. Zong, *Journal of Photochemistry and Photobiology B:*
6 *Biology*, 2014, **141**, 241-246.

7 2. Y. Q. Wang and H. M. Zhang, *Materials Research Bulletin*, 2014, **60**, 51-56.

8 3. A. Gönenç, A. Hacışevki, S. Aslan, M. Torun and B. Şimşek, *European journal of internal*
9 *medicine*, 2012, **23**, 350-354.

10 4. C. Soto, *Nature Reviews Neuroscience*, 2003, **4**, 49-60.

11 5. B. J. Yang, F. Hao, J. R. Li, D. L. Chen and R. T. Liu, *Journal of Photochemistry and*
12 *Photobiology B: Biology*, 2013, **128**, 35-42.

13 6. P. F. Qin and R. T. Liu, *Journal of hazardous materials*, 2013, **252**, 321-329.

14 7. F. Hao, M. Y. Jing, X. C. Zhao and R. T. Liu, *Journal of Photochemistry and Photobiology B:*
15 *Biology*, 2015, **143**, 100-106.

16 8. Y. Mao, M. M. Hong, A. F. Liu and D. M. Xu, *Journal of fluorescence*, 2015, **25**, 755-761.

17 9. C. M. Dai, C. W. Ji, H. X. Lan, Y. Z. Song, W. Yang and D. Zheng, *Environmental Toxicology*
18 *& Pharmacology*, 2014, **37**, 870–877.

19 10 L. Magos, S. Halbach and T. W. Clarkson, *Biochemical pharmacology*, 1978, **27**, 1373-1377.

20 11. N. J. Langford and R. E. Ferner, *Journal of human hypertension*, 1999, **13**, 651-656.

21 12. T. W. Clarkson and L. Magos, *CRC Critical Reviews in Toxicology*, 2006, **36**, 609-662.

22 13. M. K. Sharma, A. Sharma, A. Kumar and M. Kumar, *Food and chemical toxicology*, 2007, **45**,
23 2412-2419.

24 14. M. Farina, F. A. A. Soares, G. Zeni, D. O. Souza and J. B. T. Rocha, *Toxicology letters*, 2004,
25 **146**, 227-235.

26 15. D. Durak, S. Kalender, F. G. Uzun, F. Demýr and Y. Kalender, *African Journal of*
27 *Biotechnology*, 2010, **9**.

28 16. Q. Xu, Y. N. Lu, L. Y. Jing, L. J. Cai, X. F. Zhu, J. Xie and X. Y. Hu, *Spectrochimica Acta Part*
29 *A: Molecular and Biomolecular Spectroscopy*, 2014, **123**, 327-335.

30 17. W. L. DeLano, DeLano Scientific, San Carlos, CA, 2002, **452**.

31 18. A. S. Sharma, S. Anandakumar and M. Ilanchelian, *RSC Advances*, 2014, **4**, 36267-36281.

32 19. X. F. Zhang, G. Yang, Y. Dong, Y. Q. Zhao, X. R. Sun, L. Chen and H. B. Chen,
33 *Spectrochimica Acta Part A: Molecular and Biomolecular Spectroscopy*, 2015, **137**,
34 1280-1285.

35 20. A. Das and G. S. Kumar, *RSC Advances*, 2014, **4**, 33082-33090.

36 21. S. Huang, H. N. Qiu, S. Y. Lu, F. W. Zhu and Q. Xiao, *Journal of hazardous materials*, 2015,
37 **285**, 18-26.

38 22. J. R. Lakowicz, *Principles of fluorescence spectroscopy*, Springer Science & Business Media,

1   2007.

2   23.   W. R. Ware, *The Journal of Physical Chemistry*, 1962, **66**, 455-458.

3   24.   Z. X. Chi, R. T. Liu and H. Zhang, *Science of the total environment*, 2010, **408**, 5399-5404.

4   25.   J. E. N. Dolatabadi, V. Panahi-Azar, A. Barzegar, A. A. Jamali, F. Kheirdoosh, S. Kashanian

5   and Y. Omidi, *RSC Advances*, 2014, **4**, 64559-64564.

6   26.   M. Shahlaei, B. Rahimi, M. R. Ashrafi-Kooshk, K. Sadrjavadi and R. Khodarahmi, *Journal of*

7   *Luminescence*, 2015, **158**, 91-98.

8   27.   A. Belatik, S. Hotchandani, R. Carpentier and H.A. Tajmir-Riahi, *PloS one*, 2012, **7**, 1-9.

9   28.   J. Zhang, S. L. Zhuang, C. L. Tong and W. P. Liu, *Journal of agricultural and food chemistry*,

10   2013, **61**, 7203-7211.

11   29.   P. D. Ross and S. Subramanian, *Biochemistry*, 1981, **20**, 3096-3102.

12   30.   S. Tunc, O. Duman, İ. Soylu and B. K. Bozoğlan, *Journal of hazardous materials*, 2014, **273**,

13   36-43.

14   31.   Y. Shu, W. W. Xue, X. Y. Xu, Z. M. Jia, X. J. Yao, S. W. Liu and L. H. Liu, *Food chemistry*,

15   2015, **173**, 31-37.

16   32.   O. F. Sarioglu, A. Ozdemir, K. Karaboduk and T. Tekinay, *Journal of Trace Elements in*

17   *Medicine and Biology*, 2015, **29**, 111-115.

18   33.   T. Samejima, M. Kamata and K. Shibata, *Journal of biochemistry*, 1962, **51**, 181-187.

19   34.   Y. Teng, R. T. Liu, C. Li, Q. Xia and P. J. Zhang, *Journal of hazardous materials*, 2011, **190**,

20   574-581.

21   35.   Z. X. Chi, R. T. Liu, B. J. Yang and H. Zhang, *Journal of hazardous materials*, 2010, **180**,

22   741-747.

23   36.   X. F. Zhu, Y. N. Lu, J. D. Wang and Q. Xu, *Analytical Methods*, 2013, **5**, 6037-6044.

24   37.   X. R. Li, G. K. Wang, D. J. Chen and Y. Lu, *RSC Advances*, 2014, **4**, 7301-7312.

25   38.   B. Zhang, W. X. Zhai, R. T. Liu, Z. H. Yu, H. M. Shen and X. X. Hu, *Journal of Nanoscience*

26   *and Nanotechnology*, 2015, **15**, 1473-1479.

27   39.   C. Jash and G. S. Kumar, *RSC Advances*, 2014, **4**, 12514-12525.

28   40.   J. Zhang, W. X. Chen, W. Zhang, Y. Duan, Y. X. Zhu, Y. X. Zhu and Y. Zhang, *Chemical*

29   *Journal of Chinese Universities*, 2015, **36**, 1511-1516.

30   41.   S. Huang, F. W. Zhu, Q. Xiao, Q. Zhou, W. Su, H. N. Qiu, B. Q. Hu, J. R. Sheng and C. S.

31   Huang, *RSC Advances*, 2014, **4**, 36286-36300.

32   42.   X. H. Zhang, R. Q. Gao, D. P. Li, H. Y. Yin, J. L. Zhang, H. Y. Cao and X. F. Zheng,

33   *Spectrochimica Acta Part A: Molecular and Biomolecular Spectroscopy*, 2015, **136**,

34   1775-1781.

35   43.   X. L. Wei and Z. Q. Ge, *Carbon*, 2013, **60**, 401-409.

36   44.   A. Saha and V. V. Yakovlev, *Journal of biophotonics*, 2010, **3**, 670-677.

37   45.   X. R. Li, D. J. Chen, G. K. Wang and Y. Lu, *Journal of Luminescence*, 2014, **156**, 255-261.

38   46.   Y. D. Hu and L. J. Da, *Spectrochimica Acta Part A: Molecular and Biomolecular*

39   *Spectroscopy*, 2014, **121**, 230-237.

40   47.   R. Lavery and S. Sacquin-Mora, *Journal of biosciences*, 2007, **32**, 891-898.

41   48.   T. R. Griffiths and R. A. Anderson, *Canadian journal of chemistry*, 1991, **69**, 451-457.

42   49.   F. Zhang, J. Zhang, C. L. Tong, Y. D. Chen, S. L. Zhuang, and W. P. Liu, *Journal of hazardous*

1   *materials*, 2013, **263**, 618-626.

2   50.   M. S. Elgawish, N. Kishikawa, M. A. Helal, K. Ohyama and N. Kuroda, *Toxicology Research*,

3   2015, **4**, 843-847.

4   51.   R. Thakur, A. Das, V. Sharma, C. Adhikari, K. S. Ghosh and A. Chakraborty, *Physical*

5   *Chemistry Chemical Physics*, 2015, **7**, 16937-16946.

6   52.   D. Wu, J. Yan, P. X. Tang, S. S. Li, K. L. Xu and H. Li, *Food Chemistry*, 2015, **188**, 370-376.

7

1   **Table 1** Modified Stern-Volmer quenching constants and the correlation coefficient at

2   different temperatures.

T (K)	K_{sv} (L mol^{-1})	k_q (L mol^{-1} s^{-1})	R^2
295	1.03×10^{4}	1.03×10^{12}	0.992
305	5.29×10^{3}	5.29×10^{11}	0.994
315	4.43×10^{3}	4.43×10^{11}	0.994

3

4

1   **Table 2** Fluorescence lifetimes of CAT in the presence of different

2   concentrations of Hg(II).

Molar ratio of CAT to Hg(II)	τ_{AV}	χ^2
1:0	4.44	1.043
1:200	4.47	0.952
1:300	4.51	1.013
1:400	4.50	0.962
1:500	4.49	1.046

3

4

1 **Table 3** Binding constants (K_b) and binding sites (n) of the Hg(II)–CAT

2 interaction

T (K)	K_b (L moL^{-1})	n	R^2
295	13.24	0.490	0.983
305	8.90	0.508	0.973
315	8.04	0.535	0.983

3

4

1   **Table 4** Thermodynamic parameters of the Hg(II)–CAT interaction

T (K)	ΔG (KJ mol^{-1})	ΔS (J mol^{-1} K^{-1})	ΔH (KJ mol^{-1})
295	-6.23		
305	-5.78	-44.57	-19.38
315	-5.33		

2

3

1   **Table 5** CAT secondary structure contents in the presence of

2   different molar ratios of Hg(II)

Molar ratio of Hg(II) to CAT	Secondary structural elements in CAT			
	α-helix (%)	β-sheet (%)	β-turn (%)	Random coil (%)
0:1	17.6	28.9	24.1	29.7
10:1	23.6	27.4	22.2	26.9
100:1	24.7	23.6	20.8	30.4
1000:1	4.9	38.7	26.8	28.6

3

4

1   **Table 6** Docking summary of CAT with $HgCl_2$, $[HgCl_3]^-$ and $[HgCl_4]^{2-}$

	Binding Energy (kJ mol^{-1})	Van der Waals energy (kJ mol^{-1})	Electrostatic energy (kJ mol^{-1})	Inhibition Constant (mmol L^{-1})	Binding constant (L mol^{-1})
$HgCl_2$	-6.15	0.30	-6.45	83.55	11.97
$[HgCl_3]^-$	-3.06	-0.13	-2.93	292.27	3.42
$[HgCl_4]^{2-}$	-1.92	-1.17	-0.75	461.71	2.17

2

3

1   **Table 7** Distance between the amino acid residues and the Hg(II) species

Hg(II) species	Atom of the Hg(II)	Residue	Atom of the residue[a]	Distance (Å)
HgCl$_2$	Hg	Asp 395	OD	2.2
	Cl 1	Val 322	CG	3.8
	Cl 2	Glu 327	CG	3.3
	Cl 2	Val 374	CG	3.7
	Cl 2	Pro 373	CB	3.7
	Cl 2	Met 394	O	3.9
[HgCl$_3$]$^-$	Hg	Asp 24	OD	2.3
	Cl 1	Arg 381	NE	3.3
	Cl 2	Gln 21	OE	4.0
	Cl 3	Arg 18	NH	3.1
	Cl 3	Trp 14	CZ	3.7
[HgCl$_4$]$^{2-}$	Cl 1	Arg 319	NH	3.2
	Cl 2	Tyr 378	OH	3.2
	Cl 2	Pro 107	CB	3.6

2   [a] The first one character of the atom name consists of the chemical symbol for the
3   atom type. All the atom names beginning with ''C'' are carbon atoms; ''N'' indicates
4   a nitrogen and ''O'' indicates oxygen. The next character is the remoteness indicator
5   code, which is transliterated according to: "B" stands for (~) "β"; "G"~"γ"; "D"~"δ";
6   "E"~"ε"; "Z"~"ζ"; "H"~"η".

7

1
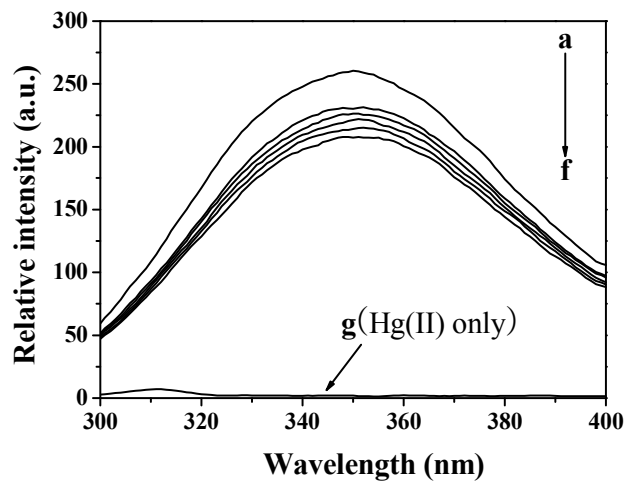
2

3   **Fig. 1** Fluorescence quenching spectra of CAT in the presence of various amounts of

4   Hg(II) (pH=7.40). c(CAT)= 1.0×10^{-6} mol L^{-1};10^{4} c(Hg(II))/(mol L^{-1}), a-f: 0, 1.0, 2.0,

5   3.0, 4.0, 5.0; g: 5.0×10^{-4} mol L^{-1} Hg(II) only.

6
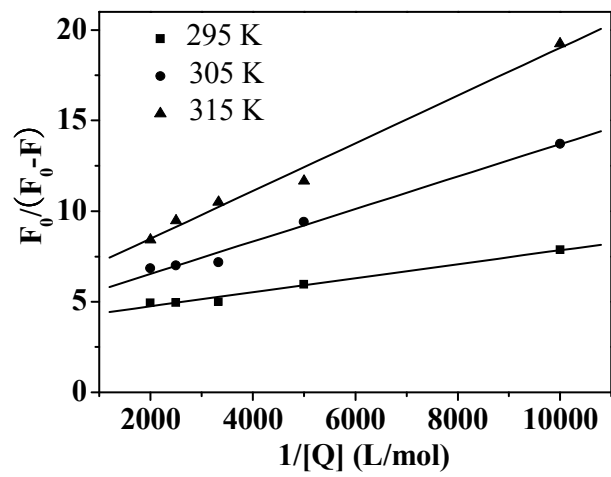
1

2   **Fig. 2** Modified Stern-Volmer plots of the Hg(II)–CAT system at three temperatures.

3
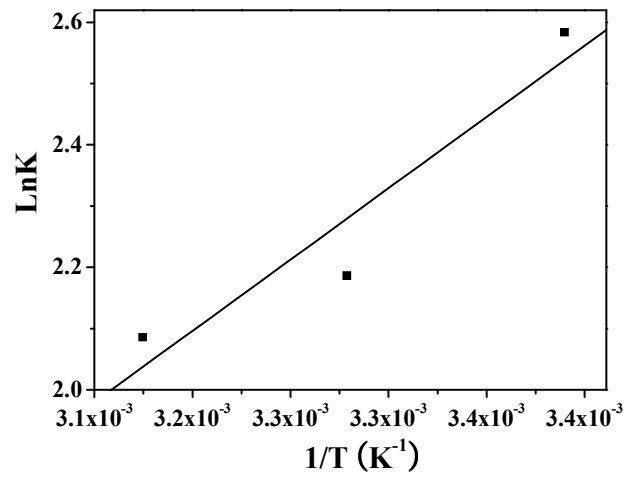
1

2   **Fig. 3** Van't Hoff plot for the interaction between Hg(II) and CAT.

3
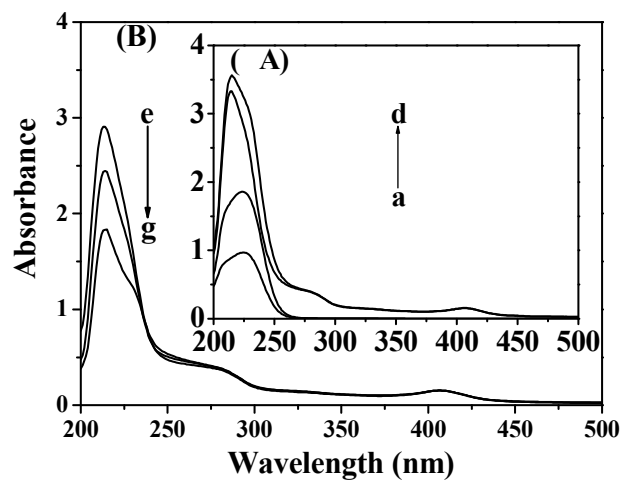
1

2   **Fig. 4** UV-vis absorption spectra of CAT in the absence and presence of different

3   concentrations of Hg(II) (pH = 7.40). Curve a: 1.0×10^{-4} mol L^{-1} Hg(II); curve b:

4   2.0×10^{-4} mol L^{-1} Hg(II); curve c: 1.0×10^{-6} mol L^{-1} CAT + 1.0×10^{-4} mol L^{-1} Hg(II);

5   curve d: 1.0×10^{-6} mol L^{-1} CAT + 2.0×10^{-4} mol L^{-1} Hg(II); curve e: 1.0×10^{-6} mol L^{-1}

6   CAT; curve f: [1.0×10^{-6} mol L^{-1} CAT + 1.0×10^{-4} mol L^{-1} Hg(II)]-[1.0×10^{-4} mol L^{-1}

7   Hg(II)]; curve g: [1.0×10^{-6} mol L^{-1} CAT + 2.0×10^{-4} mol L^{-1} Hg(II)]-[2.0×10^{-4} mol

8   L^{-1} Hg(II)].

9
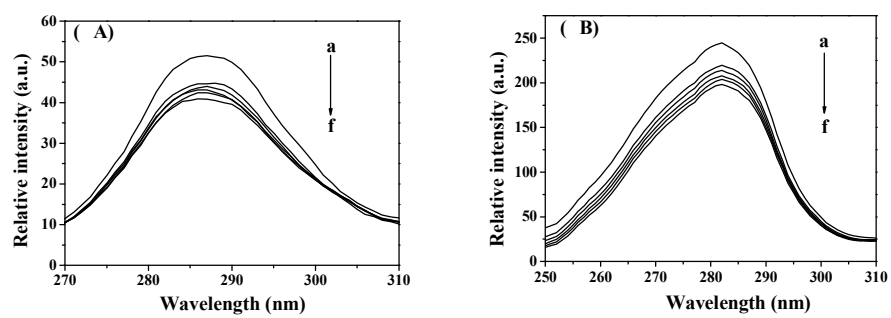
1

2   **Fig. 5** Synchronous fluorescence spectra of the Hg(II)–CAT system. (A) $\Delta\lambda$ = 15 nm;

3   (B) $\Delta\lambda$ = 60 nm. c(CAT)= 1.0×10^{-6} mol L^{-1}; $10^4\,c$(Hg(II))/(mol L^{-1}),

4   *a-f*: 0, 1.0, 2.0, 3.0, 4.0, 5.0.

5
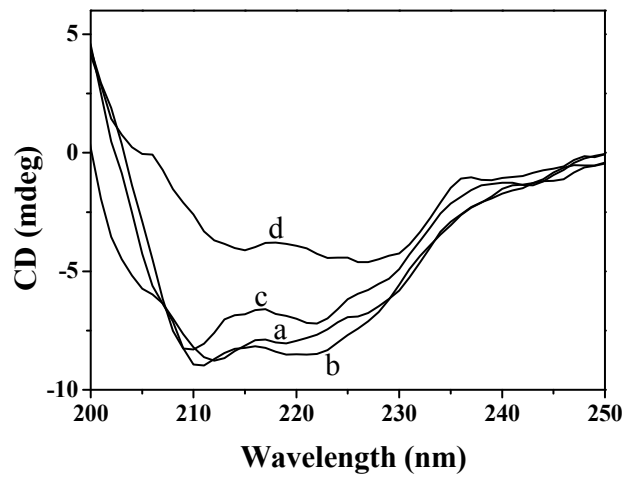
1

2   **Fig. 6** Effects of Hg(II) on the CD spectra of CAT. c(CAT)= 5.0×10^{-8} mol L^{-1};10^8

3   c(Hg(II))/(mol L^{-1}), *a-d*: 0.0, 10.0, 100.0, 1000.0.

4
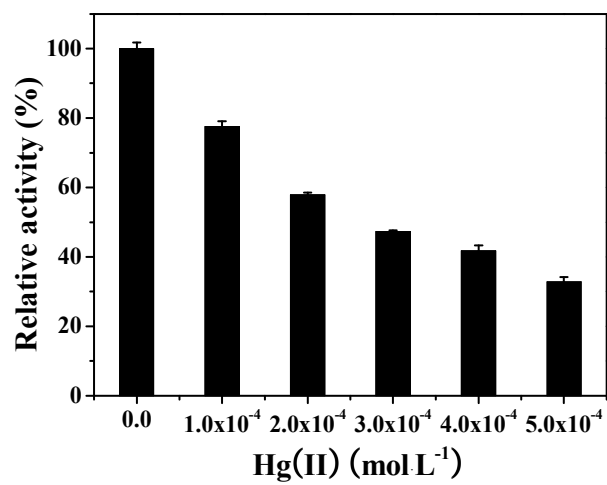
1

2   **Fig. 7** Effects of different concentrations of Hg(II) on the activity of CAT (pH =

3   7.40). c(CAT)= 1.0×10^{-6} mol L^{-1}; 10^4 c(Hg(II))/(mol L^{-1}): 0, 1.0, 2.0, 3.0, 4.0, 5.0.

4
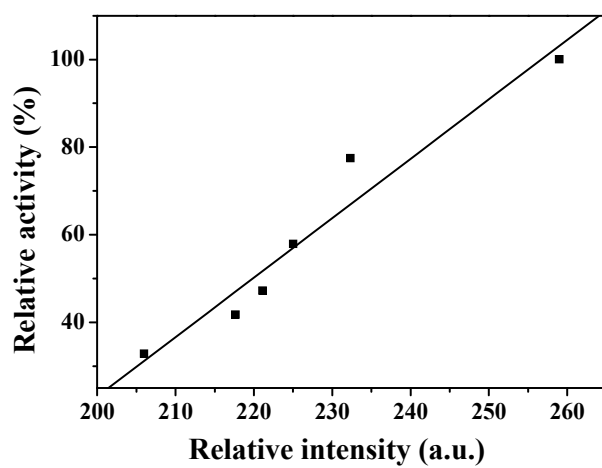
1

2   **Fig. 8** Linear relationship between the CAT activity and CAT fluorescence intensity.

3
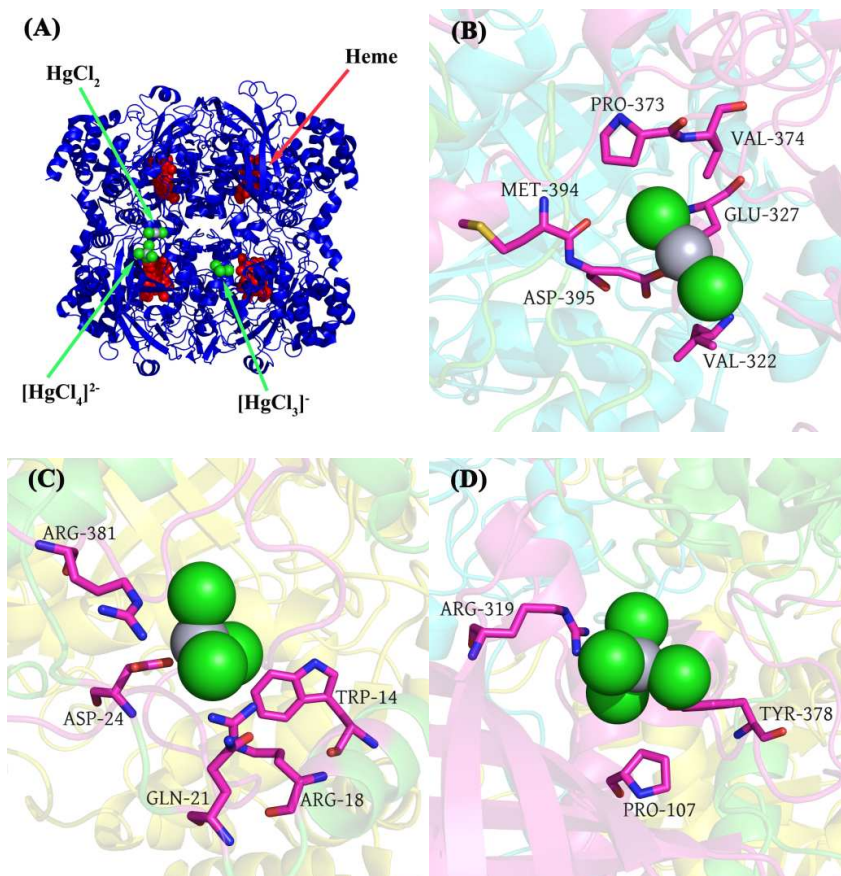
Fig. 9 Docking results of the Hg(II) and CAT system. (A) Binding sites of $HgCl_2$, $[HgCl_3]^-$ and $[HgCl_4]^{2-}$ to CAT. The interaction mode of (B) $HgCl_2$–CAT; (C) $[HgCl_3]^-$–CAT; (D) $[HgCl_4]^2$–CAT.